Bai, Ruixiang and Chen, Zhenhuan and Yan, Ceng (2007) Cross Section Design of Holey Optical Fibers with Coating Based on Stress Analysis in Tension. In *Proceedings International Conference on Mechanical Engineering and Mechanics*, pages pp. 952-955, Wuxi, China.

Cross Section Design of Holey Optical Fibers with Coating Based on Stress Analysis in Tension

Ruixiang BAI[1], Zhenhuan CHEN[1], Cheng YAN[2]

1 State Key Laboratory of Structural Analysis of Industrial Equipment, Department of Engineering Mechanics, Dalian University of Technology, Dalian, 116024, China

E-mail: bairx@dlut.edu.cn

2 School of Engineering Systems, Faculty of Built Environment and Engineering, Queensland University of Technology George St, GPO box 2434, Brisbane, QLD 4001, Australia

E-mail: c2.yan@qut.edu.au

Abstract: In this paper, the mechanical behavior of newly developed holey optical fibers with and without coating was investigated by numerical analysis. Based on experimental work, the tensile failure characteristics were observed. The stress characteristics of some typical holey fibers with different section design were studied though the finite element method under tensile load. The optimum design of air hole arrangements and sizes were proposed according to the numerical results. The influence of the coating thickness on the axial stress of holey optical fiber was also investigated. The numerical results and conclusions will be useful for the cross section optimum design of holey optical fiber for increase its strength.

Key words: Holey optical fibers; Mechanical behavior; Tensile; Coating; Finite element method

1 Introduction

Fibre is an immense improvement as a new type instrument in the modern communication filed. It just takes less than 15 years from its naissance to wide development. Its technology is beyond compare because of fast tempo, wide application and numerous subjects involved, etc. In recently years, some newly developed microstructured fiber has a promising application in telecommunication industry due to their many verified advantages, especially for the holey optical fibres which has a conventional index core surrounded by air holes and hence possesses the properties of both conventional fibres such as low transmission loss and large anomalous dispersion[1-2]. The surrounding area with holes are defined as cladding, one way to overcome pre-existing defects and to avoid further damage is to coat the surface.

In the application of fiber communication, the process of assembly is indispensably. In addition, there will be some influence result from elongating, condensation, inflect and other load effects, so in order to improve the fiber communication system work well, a comprehension understanding of its mechanical characters and failure behaviour is essential as well as its optical properties[3-5]. The mechanical properties of the holey optical fibres, as shown in Figure 1, seem to be more complicated than that of conventional silica fibre because the existence of holes not only reduces the fiber cross sectional area but also can reduce the stress intensification. This makes it important to optimize the numbers, dimension and position of the holes for increase the fiber strength.

In this paper, the discussion of cross section design of holey optical fibers with coatings in tension for the typical holey optical fibers was performed by numerical analysis. The stress analysis was executed by the commercial finite element software ANSYS. Some meaningful results were obtained.

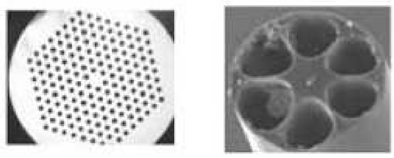

Figure 1 Cross-sections of some typical holey optical fibres

2 Definition of Section Design Parameters and Automatic Modeling Process for FEM Analysis

2.1 Definition of Section Design Parameters

Assuming a perfect manufacture, the dimensions and arrangement of the holes, the total air fraction and coating conditions are the main factors direct contribution the mechanical behaviours of holey fibers. The former is related with the local stress concentration, while the latter determines the mean stress of the section. For a typical section pattern of hexagonal lattice with one central hole missing, the diameter of holes d, pitch ^ and coating thickness t are the three main variables for section optimum as shown in Figure 2.

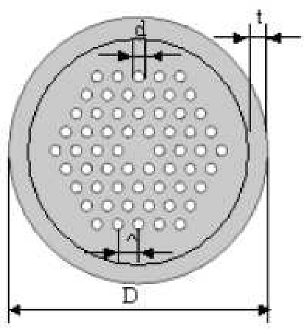

Figure 2 Definition of section design parameters

2.2 Automatic Modeling Process for Fem Analysis

For a certain value of Diameter D and air fraction Ψ%, the diameter of holes d can be determined as follows

For one central hole missing

$$d = D\sqrt{\frac{\psi\%}{3n(n+1)}} \tag{1}$$

Where n denote the number of rings.

The geometric limit of pitch ∧ is

$$\Lambda > d \tag{2}$$

For the section pattern with a large air fraction shown as Fig.8-c

$$d = D\sqrt{\frac{\psi\%}{6}} \tag{3}$$

The geometric limit of pitch ∧ is

$$d < \Lambda < (D-d)/2 \tag{4}$$

Thus, for a given value of D and Ψ%, by varying the value of d and ∧, we can get different patterns of cross section designs. Using the finite element software ANSYS to make a comprehensive stress analysis, enough models of holey fibers with different cross sections are needed. If we build these modes manually, it means a heavy work. We use the parametric design language APDL provided by ANSYS to build the models automatically and to automate common tasks in terms of parameters, which brought a great convenience for current analysis.

Only one sixth of the structure was calculated due to the periodic symmetry of the section, and the element type of SOLID185 was used in current analysis. Since the main purpose of this section is to make a comparison of stress condition under different cross section designs, thus a moderately scale of mesh precision is competent to do the work. While the scale of mesh precision should be kept consistent for all the models, taking full length of samples for calculation is not necessary, the length of 10mm for all the fibers are taken into account, and the segments of finite element models are shown in Figure 3.

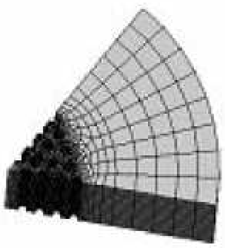

Figure 3 Scheme of meshing controls

2.3 Load and Boundary Condition

Two different boundary conditions are considered, namely one end face bonded and one side face bonded as shown in Figure 4, the tensile load was applied on the free end in a uniform pattern.

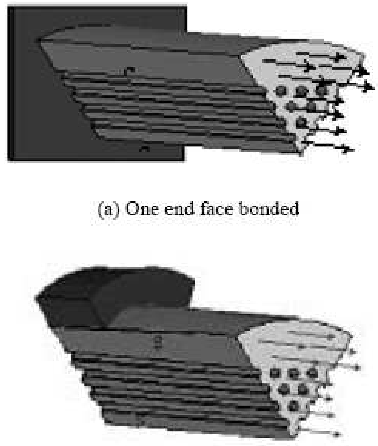

(a) One end face bonded

(b) One side face bonded

Figure 4 Load and Boundary Condition

3 Results and discussion

3.1 Stress distribution

For the holy fibre with four rings holes, the total axial tensile load applied in a uniform pattern was 10N. The material properties of silica are E=70.3 GPa, ν=0.17, and for that of coating material is E=3.96 GPa, ν=0.39. D=125μm, Λ=10μm, t=60μm and air fraction Ψ%=10%.. The contour plot of axial stress σ_z under boundary condition of one end face bonded near end face can be seen in Figure 5 and Figure6. Since the axial stress σ_z is greater than other stress component for several orders of magnitude, here we just mention axial stress σ_z.

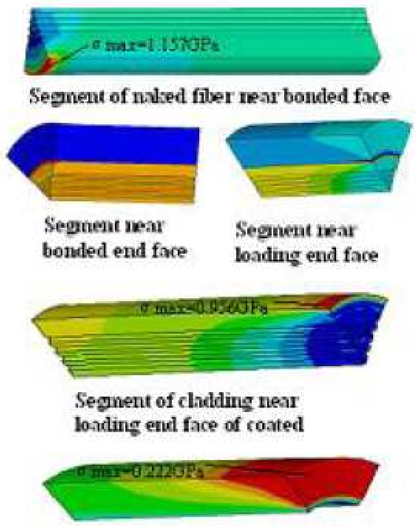

Figure 5 Stress distribution of naked and coated fiber under one end face bonded

Figure 5 and Figure 6 also show the contour plot of axial stress σ_z of naked fiber with same length and load. For naked fiber under the two different boundary conditions, the high stress areas present only near the constrained zones, out of this range, the axial stress σ_z present in a uniform state. While for the coated fibers, the high stress areas present both near the constrained zones and loading face, and for most area away form these two regions, the axial stress σ_z presents in a uniform state. The highest stress presents in the cladding. For the coating polymer, the comparative high stress region presents near the loading end or side, and for the case of side bonded condition, another comparative high stress region also can be seen near the edge between the constrained area and the free area.

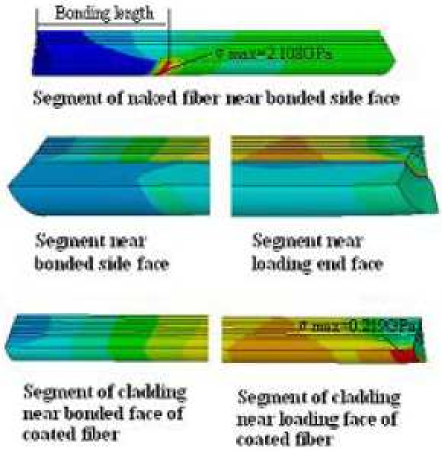

Figure 6 Stress distribution of naked and coated fiber under one side face bonded

4 Discussion of Section Design Parameters

Experiment investigation has proved that the tensile behaviour of all samples was closely associated with how the fibre was gripped. In addition to this, the section parameters such as the diameter of holes d pitch ^ and coating thickness t are also considered to be essential factors affecting the failure load of the fiber. As shown in Figure 7, we take four different typical patterns with holes of three to six rings marked with P1, P2, P3 and P4, respectively.

Figure 7 Four different section types with holes of 3-6 rings

4.1 Effect of polymer coating thickness t on nondimensional maximum axial stress

Keep D=125μm, Λ=10μm and air fraction Ψ%=10%. The boundary condition is one end face bonded. Figure 8 shows the results of nondimensional maximum axial stress $\sigma_z^{\max} / \sigma_{zrod}^{\max}$ varies with coating radius, where $\sigma_{zrod}^{\max}$ is the maximum axial stress of naked silica rod with same net section area as naked holey fiber under the same loading and boundary condition.

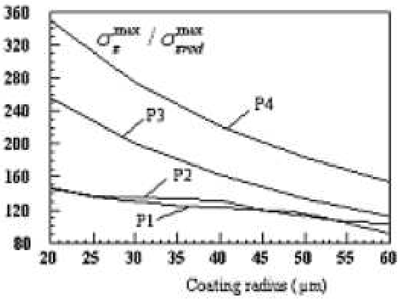

Figure 8 Nondimensional stresses vs. coating thickness

From Figure 8, it can be seen that the nondimensional maximum axial stresses are all decreased with the increasing of coating thickness, and the maximum axial stresses in fiber with holes of five rings and six rings decrease more obviously than that of fiber with holes of three rings and four rings, when the coating thickness reach 60μm, these two curves tend to be flat. For section pattern P3, Figure 9 gives the results under two different boundary conditions of end face bonded and side face bonded, and the two curves in Figure 10 has a similar variation tendency, namely the maximum axial stress will decrease with the increasing of coating thickness. From the results shown in figure 8 and figure9 we can see that for different cross section patterns, the coating thickness can be optimized for an ideal value.

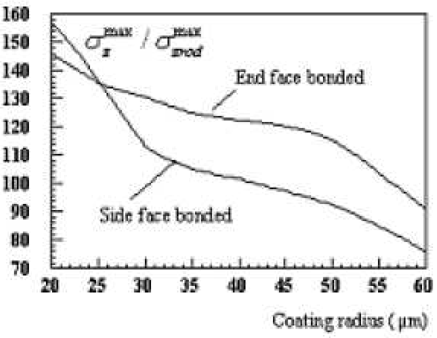

Figure 9 Nondimensional stresses vs. coating thickness of P3 under different boundary conditions

4.2 Effect of pitch on the nondimensional maximum axial stress

Keep D=125μm, t=10μm and air fraction Ψ%=10%. The boundary condition is one end face bonded. Figure 10 shows the results of nondimensional maximum axial stress varies with pitch ^ of holes. The curves illustrate that for section type P3, the influence of pitch is not as prominent as that of other section types, while for the section type P2 and P4, when the value of pitch ^ exceeds 8.5μm, the maximum axial stress will increased severely. In present loading and boundary condition, the suitable range of pitch ^ is about 8μm to 9μm.

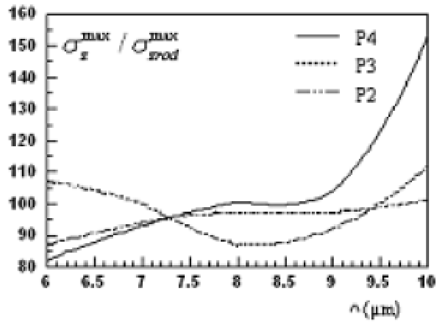

Figure 10 Nondimensional stress vs. pitch for different section patterns as one end face bonded

4.3 Comparison of nondimensional maximum axial stress with holes of 3-6 rings

To make a comparison of maximum axial stress with different hole radius should keep the same air fraction Ψ in order to have same net cross section area, thus if the hole radius changes, the rings of holes should also be changed. Table 1 shows the maximum axial stress of fiber with four different section patterns under the same air fraction when one end face bonded. From table 1, it can be seen that the fiber with section pattern of four rings holes has a comparatively low maximum axial stress in current loading and boundary condition.

Table 1 Normalized stress (core=10, coat=60, Ψ%=10%)

Section pattern	P1	P2	P3	P4
Normalized stress	103.3	90.7	112.2	153.2

5 Conclusion

The stress distribution characteristic of holey optical fiber was investigated, and the influence of cross section parameters on the axial stress was discussed. The stress distribution characteristic of coated holey optical fiber is quite different from that of the naked fiber. If neglect the defects, the axial stress segment away from constraint and loading site presents in a uniform state when tensile load was applied, while for the segment near constraint or loading site, a high stress zone exists. An optimum design of cross section parameters such as the diameter of holes, pitch and coating thickness can decrease the value of high maximum stress.

Acknowledgment

The authors are grateful to the support of Australian Research Council Discovery Project Fellowship.

References

[1] N GUAN, K IZOE, K TAKENAGA, R SUZUKI, K AIKAWA, KHIMENO. Holey Fibers for low bending loss. IEICE Trans. Electron. 2006. No. 2: 191-196

[2] B YAO, O Kazumasa, k Yoshinori, K TomoyoshI, T Masao. Low-loss Holey Fiber. HItachi Cable Review, 2005. No.24: 1-5

[3] A SKONTORP. Strength and failure mechanisms of polyimide-coated optical fibers. In Smart structures and materials 2000: Sensory phenomena and measurement instrumentation for smart structures and materials, Proceedings of SPIE, 2000. Vol.3986, 240-251

[4] R J HAND, B EllIS, B R WHITTLE, F H Wang. Epoxy based coatings on glass:strengthening mechanisms. Journal of Non-Crystalline Solids, 2003. No. 315: 276-287

[5] S L SEMJONOV, C R KURKJIAN. Strengh of silica optical fibers with micron size flaws. Joural of Non-crystalline Solids, 2001. No. 283: 220-224